

Noise properties of superconducting coplanar waveguide microwave resonators

Jiansong Gao^{a)} and Jonas Zmuidzinas

Physics Department, California Institute of Technology, Pasadena, California 91125

Benjamin A. Mazin, Henry G. LeDuc, and Peter K. Day

Jet Propulsion Laboratory, California Institute of Technology, Pasadena, California 91109

(Received 20 September 2006; accepted 1 February 2007; published online 8 March 2007)

The authors have measured noise in thin-film superconducting coplanar waveguide resonators. This noise appears entirely as phase noise, equivalent to a jitter of the resonance frequency. In contrast, amplitude fluctuations are not observed at the sensitivity of their measurement. The ratio between the noise power in the phase and amplitude directions is large, in excess of 30 dB. These results have important implications for resonant readouts of various devices such as detectors, amplifiers, and qubits. They suggest that the phase noise is due to two-level systems in dielectric materials.

© 2007 American Institute of Physics. [DOI: 10.1063/1.2711770]

Thin-film superconducting microwave resonators are of interest for a number of applications, including the multiplexed readout of single electron transistors,¹ microwave kinetic inductance detectors (MKIDs),^{2,3} normal metal-insulator-superconductor tunnel junction detectors,⁴ superconducting quantum interference devices,^{5,6} and qubits.^{7,8} The device to be measured presents a variable dissipative or reactive load to the resonator, influencing the resonator quality factor Q_r or frequency f_r , respectively. Changes to both Q_r and f_r may be determined simultaneously by sensing the amplitude and phase of a microwave probe signal.² While several early demonstrations used hand-assembled lumped-element circuits,^{1,4,5} frequency-domain multiplexing of large arrays generally will require compact microlithographed high- Q_r resonators.¹ Such resonators are also needed for strong coupling to charge qubits.⁷ Noise in microlithographed resonators has been observed^{2,3} and can be a limiting factor for device performance but is not well understood. In this letter, we report measurements of resonator noise, show how the noise spectra separate into amplitude and phase components, and discuss the physical origin of the noise.

We studied quarter-wavelength coplanar waveguide (CPW) resonators² [Fig. 1(a)] with center strip widths w of 0.6–6 μm and gaps g between the center strip and ground planes of 0.4–4 μm , and with impedances $Z_0 \approx 50 \Omega$. Resonator lengths of 3–7 mm produce resonance frequencies f_r between 4 and 10 GHz. Frequency multiplexed arrays of up to 100 resonators are coupled to a single CPW feedline. The CPW circuits are patterned from a film of either Al ($T_c = 1.2 \text{ K}$) or Nb ($T_c = 9.2 \text{ K}$) on a crystalline substrate, either sapphire, Si, or Ge. The surfaces of the semiconductor substrates are not intentionally oxidized, although a native oxide due to air exposure is expected to be present.

A microwave synthesizer at frequency f is used to excite a resonator. The transmitted signal is amplified with a cryogenic high electron mobility transistor (HEMT) amplifier and is compared to the original signal using an IQ mixer, whose output voltages I and Q are proportional to the in-phase and quadrature amplitudes of the transmitted signal^{2,3} (see Fig. 2 inset). As f is varied, the output $\xi = [I, Q]^T$ (the superscript T

represents the transpose) traces out a resonance circle [Fig. 1(b)]. With f fixed, ξ is seen to fluctuate about its mean, and the fluctuations $\delta\xi(t) = [\delta I(t), \delta Q(t)]^T$ are digitized for noise analysis, typically over a 10 s interval using a sample rate of 250 kHz.

The fluctuations $\delta\xi(t)$ are observed to be primarily in the direction tangent to the resonance circle, while the fluctuations in the orthogonal direction are small. These two directions correspond to fluctuations in the phase and amplitude of the resonator's electric field \mathbf{E} , respectively. This observation can be quantified by studying the spectral-domain noise covariance matrix $S(\nu)$ defined by

$$\langle \delta\xi(\nu) \delta\xi^\dagger(\nu') \rangle = S(\nu) \delta(\nu - \nu'), \quad S(\nu) = \begin{pmatrix} S_{II}(\nu) & S_{IQ}(\nu) \\ S_{IQ}^*(\nu) & S_{QQ}(\nu) \end{pmatrix}, \quad (1)$$

where $\delta\xi(\nu)$ is the Fourier transform of the time-domain data, the dagger represents the Hermitian conjugate, $S_{II}(\nu)$ and $S_{QQ}(\nu)$ are the autopower spectra, and $S_{IQ}(\nu)$ is the

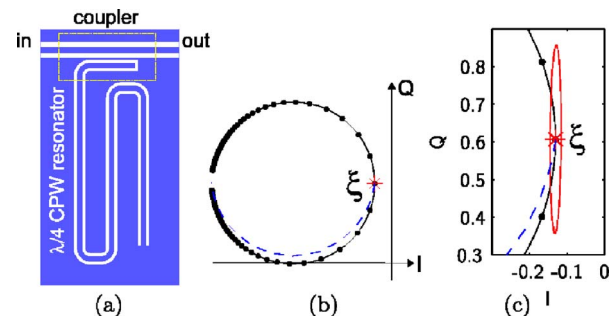


FIG. 1. (Color online) (a) Schematic illustration (not to scale) of the resonator and feedline geometry; See Day *et al.* (Ref. 2) for the equivalent circuit. Black represents the superconducting film and white represents bare substrate. The coupler relies on the mutual capacitance between the center strips of the feedline and resonator CPW lines and may be considered to be a lumped element $C = 1/(f_r Z_0 \sqrt{8\pi Q_c})$, where Q_c is the coupling-limited quality factor. (b) Resonance circle of a 200 nm Nb on Si resonator at 120 mK (solid line), quasiparticle trajectory calculated from Mattis-Bardeen theory (Ref. 10) (dashed line). For this figure, the readout point $\xi = [I, Q]$ is located at the resonance frequency f_r . (c) Noise ellipse (magnified by a factor of 30). Other parameters are $f_r = 4.35 \text{ GHz}$, $Q_r = 3.5 \times 10^5$ (coupling limited), $w = 5 \mu\text{m}$, $g = 1 \mu\text{m}$, readout power $P_r \approx -84 \text{ dBm}$, and internal power $P_{\text{int}} \approx -30 \text{ dBm}$.

^{a)}Electronic mail: jiansong@caltech.edu

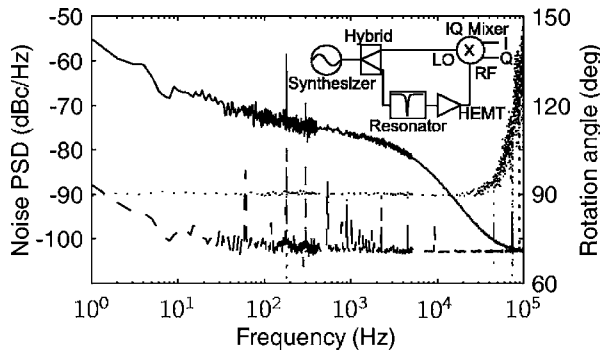


FIG. 2. Noise spectra in the phase [$S_{aa}(\nu)$, solid line] and amplitude [$S_{bb}(\nu)$, dashed line] directions, and the rotation angle [$\phi(\nu)$, dotted line]. The noise data are from the same Nb/Si resonator under the same condition as in Fig. 1. The inset shows the diagram of the homodyne readout system.

cross-power spectrum. The matrix $S(\nu)$ is Hermitian and may be diagonalized using a unitary transformation; however, we find that the imaginary part of S_{IQ} is negligible and that an ordinary rotation applied to the real part $\text{Re} S(\nu)$ gives almost identical results. The eigenvectors and eigenvalues are calculated at every frequency ν ,

$$O^T(\nu)\text{Re} S(\nu)O(\nu) = \begin{pmatrix} S_{aa}(\nu) & 0 \\ 0 & S_{bb}(\nu) \end{pmatrix}, \quad (2)$$

where $O(\nu)=[v_a(\nu), v_b(\nu)]$ is an orthogonal rotation matrix. We use $S_{aa}(\nu)$ and $v_a(\nu)$ to denote the larger eigenvalue and its eigenvector.

A typical pair of spectra $S_{aa}(\nu)$ and $S_{bb}(\nu)$ shown in Fig. 2, along with the rotation angle $\phi(\nu)$, defined as the angle between $v_a(\nu)$ and the I axis. Three remarkable features are found for all noise data. First, $\phi(\nu)$ is independent of ν within the resonator bandwidth (the rms scatter is $\sigma_\phi \leq 0.4^\circ$ per 10 Hz frequency bin from 1 Hz to 5 kHz), which means that only two special directions, v_a and v_b , diagonalize $S(\nu)$. Equation (2) shows that $S_{aa}(\nu)$ and $S_{bb}(\nu)$ are the noise spectra projected into these two constant directions. Second, v_a is always tangent to the IQ resonance circle while v_b is always normal to the circle, even when f is detuned from f_r . Third, $S_{aa}(\nu)$ is well above $S_{bb}(\nu)$ (see Fig. 2). The character of the noise can be clearly visualized by plotting a noise ellipse, defined by $\delta\xi^T C^{-1} \delta\xi = 1$, where $C = \int_{\nu_1}^{\nu_2} \text{Re} S(\nu) d\nu$ is the covariance matrix for δI and δQ filtered for the corresponding bandpass (we use $\nu_1 = 1$ Hz and $\nu_2 = 1$ kHz). The major axis of the noise ellipse is always in the phase direction, and the ratio of the two axes is always very large [Fig. 1(c)].

Figure 2 also shows that the amplitude noise spectrum is flat except for a $1/\nu$ knee at low frequency contributed by the electronics. The amplitude noise is independent of whether the synthesizer is tuned on or off the resonance and is consistent with the noise temperature of the HEMT amplifier. The phase noise spectrum⁹ has a $1/\nu$ slope below 10 Hz, typically a $\nu^{-1/2}$ slope above 10 Hz, and a roll off at the resonator bandwidth $f_r/2Q_r$. The phase noise is well above the HEMT noise, usually by two or three orders of magnitude (in rad^2/Hz) at low frequencies. It is well in excess of the synthesizer phase noise contribution or the readout system noise.^{2,3}

Quasiparticle fluctuations in the superconductor can be securely ruled out as the source of the measured noise by

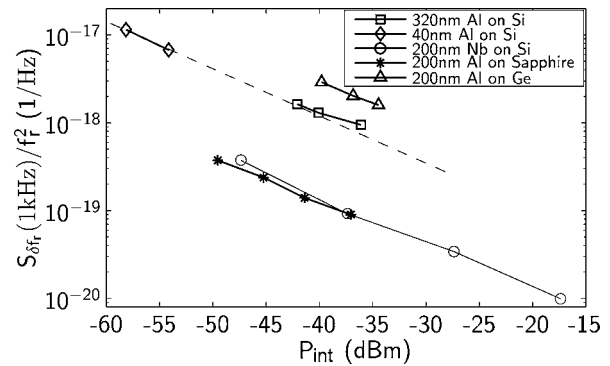


FIG. 3. Power and material dependence of the phase noise at $\nu = 1$ kHz. To compare resonators with different f_r and Q_r , phase noise is converted to fractional frequency noise, calculated by $S_{\delta f_r}(\nu)/f_r^2 = S_{aa}(\nu)/4Q_r^2$. All the resonators have $w = 3 \mu\text{m}$ and $g = 2 \mu\text{m}$ and are measured around 120 mK.

considering the direction in the IQ plane that would correspond to a change in quasiparticle density δn_{qp} . Both the real and inductive parts of the complex conductivity σ respond linearly to δn_{qp} , $\delta\sigma = \delta\sigma_1 - i\delta\sigma_2$, resulting in a trajectory that is always at a nonzero angle $\psi = \tan^{-1}(\delta\sigma_1/\delta\sigma_2)$ to the resonance circle, as indicated by the dashed lines in Figs. 1(b) and 1(c). Mattis-Bardeen¹⁰ calculations yield $\psi > 7^\circ$ for Nb below 1 K, so quasiparticle fluctuations are strongly excluded since $\psi \gg \sigma_\phi$. Furthermore, ψ is measured experimentally by examining the response to x-ray, optical/UV, or sub-millimeter photons and is typically $\psi \approx 15^\circ$.¹¹

The phase noise depends on the microwave power inside the resonator (P_{int}), the materials used for the resonator, and the operating temperature. The power dependence for various material combinations is shown in Fig. 3; all follow the scaling $S_{aa}(\nu) \propto P_{\text{int}}^{-1/2}$. For comparison, amplifier phase noise is a multiplicative effect that would give a constant noise level independent of P_{int} , while the amplifier noise temperature is an additive effect that would produce a $1/P_{\text{int}}$ dependence. Sapphire substrates generally give lower phase noise than Si or Ge. However, the Nb/Si device showed low noise comparable with Al/sapphire, suggesting that the etching or interface chemistry, which is different for Nb and Al, may play a role. Two Al/Si resonators with very different Al thicknesses and kinetic inductance fractions¹² fall onto the dashed equal-noise scaling line, strongly suggesting that the superconductor is not responsible for the phase noise.³ Furthermore, the noise of a Nb/Si resonator decreased by a factor of 10 when warmed from 0.2 to 1 K, stronger evidence against superconductor noise since Nb has $T_c = 9.2$ K and its properties change very little for $T \ll T_c$. More detail on the temperature dependence will be published separately.

The evidence leads us to suggest that the noise is caused by fluctuating two-level systems (TLSs) in the dielectric materials—either the bulk substrate or its exposed surface, the interface layers between the metal films and the substrate, or any oxide layers on the metal surfaces. Models assuming a collection of TLS with a wide range of excitation energies E and relaxation rates have long been used to explain the low temperature physical properties of noncrystalline solids.^{13–15} TLSs are also found in crystalline materials^{16,17} but at lower densities. Fluctuations due to TLS are of interest theoretically^{18,19} and have been observed in dielectrics, either as telegraph or $1/\nu$ noise, using tunnel junctions,²⁰ single electron transistors,²¹ and atomic force microscopes.²² Other examples include telegraph noise in the resistance of metallic

nanoconstrictions²³ and qubit dephasing effects.⁸

Recent experiments^{7,24} have illustrated the reactive loading effect that occurs when a single TLS (a qubit) is coupled to a microwave resonator. For weak coupling g or large detuning $\Delta f = |E/\hbar - f_r|$, $g \ll \Delta f$, this reactive loading causes the resonator frequency to shift by $\pm g^2/\Delta f$ depending on the quantum state of the TLS. Thermal fluctuations—absorption or emission of thermal phonons by a collection of TLS—could therefore cause phase noise, equivalent to a fluctuating dielectric constant $\delta\epsilon(\mathbf{r}, t)$. For this model one expects the noise to vanish exponentially for $T \ll \hbar f_r/2k$ as the TLSs settle into their ground states, while the increase in TLS-phonon transition rates might explain the observed noise decrease at high temperatures. However, at present we do not have a model which quantitatively explains the data. Alternatively, TLS frequency fluctuations $\delta E(t)/\hbar$ produced by TLS-TLS interactions^{15,25} and observed in single molecule optical fluorescence experiments^{26,27} should give phase noise with a power law rather than exponential decrease at low temperatures.

The $P_{\text{int}}^{-1/2}$ noise scaling is indicative of TLS saturation; otherwise, the phase noise would be independent of P_{int} as expected for dielectric constant fluctuations. Similarly, power-independent thermal fluctuations of the TLS dielectric polarization $\delta\mathbf{P}^{19}$ are ruled out since this would give additive noise with equal amplitude and phase components and scaling as $1/P_{\text{int}}$. TLS saturation effects are well known;^{8,15} indeed, f_r and Q_r show anomalous temperature and power dependence²⁸ for $T \ll T_c$. Saturation of a single TLS depends on its frequency detuning Δf , its position \mathbf{r} in the spatially varying resonator field $\mathbf{E}(\mathbf{r})$, and the orientation and strength of its dipole moment \mathbf{d} . The growth of the saturation zone in this parameter space with increasing P_{int} may explain the observed $P_{\text{int}}^{-1/2}$ noise scaling.

The microwave fields in our resonators are sufficiently strong to cause TLS saturation. In the Bloch equation framework, saturation for zero detuning occurs when $\Omega^2 T_1 T_2 > 1$, where $\Omega = \mathbf{d} \cdot \mathbf{E}/\hbar$ is the Rabi frequency and T_1^{-1} , T_2^{-1} are the usual energy relaxation and dephasing rates.²⁹ The distribution of T_1^{-1} is extremely broad,¹⁵ extending above and below the range of noise frequencies we observe, because $T_1^{-1} \propto \Delta_0^2/E^2$ is controlled by the tunnel coupling Δ_0 and is therefore exponentially sensitive to the potential barrier.^{15,29} For silica, $T_1^{-1} \approx 1$ MHz $(E/4 \text{ GHz})^3 (\Delta_0/E)^2 \coth(E/2kT)$. The dipole moment \mathbf{d} is proportional to Δ_0/E ,¹⁵ so $\Omega^2 T_1$ is independent of Δ_0 . Meanwhile, T_2^{-1} scales as $(1 - \Delta_0^2/E^2)$ (Ref. 15 and 29) and has a relatively narrow distribution; for silica, $T_2^{-1} \approx 10$ MHz $(T/200 \text{ mK})^{1.5}$.³⁰ Saturation is therefore mostly independent of Δ_0 and occurs when $\mathbf{E} \cdot \mathbf{d}/|\mathbf{d}|$ exceeds a critical value $E_c(f_r, T)$. Indeed, the shape of the observed phase noise spectrum does not change significantly with P_{int} until the superconductors become nonlinear.³ For silica, $E_c(4 \text{ GHz}, 200 \text{ mK}) \approx 31 \text{ V m}^{-1}$ and corresponds to $P_{\text{int}} \approx -75 \text{ dBm}$ which is significantly below the power levels we use (see Fig. 3). We also find $E_c(7.2 \text{ GHz}, 25 \text{ mK}) \approx 10 \text{ V m}^{-1}$, which is appropriate for the experimental conditions of Martinis *et al.*⁸ and is similar to their observed onset of TLS saturation.

In summary, we find that lithographed resonators display $\nu^{-1/2}$ noise directed purely in the phase direction which varies with readout power, temperature, and the substrate material. These results are important for the device

optimization—devices relying on resistive loading should be able to avoid this noise source. For MKIDs, the $\sin \psi$ amplitude component of the signal is already available when using an IQ readout, and an optimally weighted phase/amplitude measurement can substantially improve the sensitivity at low frequencies where the phase noise is larger.

The authors thank Sunil Golwala, Kent Irwin, Andrew Lange, Konrad Lehnert, John Martinis, and Harvey Moseley for useful discussions. This work was supported in part by the NASA Science Mission Directorate, JPL, Gordon and Betty Moore Foundation, and Alex Lidow, a Caltech Trustee.

¹T. R. Stevenson, F. A. Pellerano, C. M. Stahle, K. Aidala, and R. J. Schoelkopf, Appl. Phys. Lett. **80**, 3012 (2002).

²P. K. Day, H. G. LeDuc, B. A. Mazin, A. Vayonakis, and J. Zmuidzinas, Nature (London) **425**, 817 (2003).

³B. A. Mazin, Ph.D. thesis, Caltech, 2004.

⁴D. R. Schmidt, C. S. Yung, and A. N. Cleland, Appl. Phys. Lett. **83**, 1002 (2003).

⁵K. D. Irwin and K. W. Lehnert, Appl. Phys. Lett. **85**, 2107 (2004).

⁶I. Hahn, B. Bumble, H. Leduc, M. Weilert, and P. Day, AIP Conf. Proc. **850**, 1613 (2006).

⁷A. Wallraff, D. I. Schuster, A. Blais, L. Frunzio, R.-S. Huang, J. Majer, S. Kumar, S. M. Girvin, and R. J. Schoelkopf, Nature (London) **431**, 162 (2004).

⁸J. M. Martinis, K. B. Cooper, R. McDermott, M. Steffen, M. Ansmann, K. D. Osborn, K. Cicak, S. Oh, D. P. Pappas, R. W. Simmonds, and C. C. Yu, Phys. Rev. Lett. **95**, 210503 (2005).

⁹The phase noise spectra we present are conceptually different from those commonly used to represent the phase noise of active oscillators or frequency sources. Our noise spectra refer to a passive resonator driven at fixed frequency; in this case, a resonance frequency shift δf_r causes a proportional phase shift $\delta\theta = 2Q_r \delta f_r / f_r$ in the resonator field. In contrast, if we locked an active oscillator to our passive resonator, the oscillator's output phase shift relative to a perfect clock would now be the time integral of $2\pi \delta f_r(t)$, and we would therefore observe an extra $1/\nu^2$ factor in the oscillator's phase noise spectrum at low frequencies.

¹⁰D. C. Mattis and J. Bardeen, Phys. Rev. **111**, 412 (1958).

¹¹B. A. Mazin, B. Bumble, P. K. Day, M. E. Eckart, S. Golwala, J. Zmuidzinas, and F. A. Harrison, Appl. Phys. Lett. **89**, 222507 (2006).

¹²J. Gao, J. Zmuidzinas, B. A. Mazin, P. K. Day, and H. G. Leduc, Nucl. Instrum. Methods Phys. Res. A **559**, 585 (2006).

¹³P. W. Anderson, B. I. Halperin, and C. M. Varma, Philos. Mag. **25**, 1 (1972).

¹⁴W. A. Phillips, J. Low Temp. Phys. **7**, 351 (1972).

¹⁵W. A. Phillips, Rep. Prog. Phys. **50**, 1657 (1987).

¹⁶R. N. Kleiman, G. Agnolet, and D. J. Bishop, Phys. Rev. Lett. **59**, 2079 (1987).

¹⁷W. A. Phillips, Phys. Rev. Lett. **61**, 2632 (1988).

¹⁸C. C. Yu, J. Low Temp. Phys. **137**, 251 (2004).

¹⁹A. Shnirman, G. Schon, I. Martin, and Y. Makhlin, Phys. Rev. Lett. **94**, 127002 (2005).

²⁰R. T. Wakai and D. J. Van Harlingen, Phys. Rev. Lett. **58**, 1687 (1987).

²¹A. B. Zorin, F.-J. Ahlers, J. Niemeyer, T. Weimann, and H. Wolf, Phys. Rev. B **53**, 13682 (1996).

²²L. Walther, E. Vidal Russel, N. Israeloff, and H. Alvarez Gomariz, Appl. Phys. Lett. **72**, 3223 (1998).

²³K. S. Ralls and R. A. Buhrman, Phys. Rev. Lett. **60**, 2434 (1988).

²⁴D. I. Schuster, A. Wallraff, A. Blais, L. Frunzio, R.-S. Huang, J. Majer, S. M. Girvin, and R. J. Schoelkopf, Phys. Rev. Lett. **94**, 123602 (2005).

²⁵J. L. Black and B. I. Halperin, Phys. Rev. B **16**, 2879 (1977).

²⁶W. P. Ambrose and W. E. Moerner, Nature (London) **349**, 225 (1991).

²⁷A. M. Boiron, P. Tamarat, B. Lounis, R. Brown, and M. Orrit, Chem. Phys. **247**, 119 (1999).

²⁸R. Barends, J. J. A. Baselmans, J. N. Hovenier, J. R. Gao, S. J. C. Yates, T. M. Klapwijk, and H. F. C. Hoevers, IEEE Trans. Appl. Supercond. (submitted).

²⁹F. K. Wilhelm, M. J. Storcz, U. Hartmann, and M. R. Geller, *Manipulating Quantum Coherence in Solid State Systems*, NATO-ASI Series, edited by M. Flatte and I. Tifrea (Springer, Dordrecht, in press).

³⁰W. O. Putikka and D. L. Huber, Phys. Rev. B **36**, 3436 (1987).